CORROSION PROBLEMS IN AIRCRAFT COMPONENTS--

CASE STUDIES OF FAILURES

W. R. Coleman, R. J. Block and R. D. Daniels
University of Oklahoma
Norman, Oklahoma 73019

Abstract

Case histories describing the analysis of failures of aircraft engine and accessory components are presented. In each case corrosion is identified as a causative or contributive factor to the failures.

Failures of cartridge pneumatic starter breech chambers have been observed in a number of jet engines. The failures are usually attended by significant damage to the aircraft. Failure analysis is often made difficult by excessive flame erosion of the fracture surfaces. Stress corrosion cracking, induced by residual or thermal stresses and the presence of corrosive combustion products, was observed in a breech chamber made of 4340 steel. Failure appears to have been the consequence of the geometry of the component coupled with use of a medium alloy steel in an extremely hostile environment.

An in-flight failure of the engine tail cone from an A-7D aircraft involved the loss of about one-third of the length of the assembly. The potential danger associated with an in-flight separation of several feet of metal tube is immediately obvious. The cone was fabricated from A-286 alloy. Failure originated at the junction between a longitudinal seam and a circumferential weld which joined a stiffener to the outside of the cone. Evidence of thermal and ordinary fatigue was noted and stress corrosion cracking in the weld nugget and base metals was documented.

Bursting of a 2024 aluminum hydraulic cylinder barrel on the inner landing gear door actuator of an F-101 aircraft was the result of fatigue and overload. However, the failure was found to have been induced by surface pitting. The failure initiated beneath an identification band which encircled the component. Similar failures have been observed in the main landing gear actuating cylinders of C-141 aircraft (2014 aluminum). Placing tightly fitting bands on such components appears to invite corrosion due to differential aeration. The pitting induced by crevice type corrosion sufficiently elevates the stresses locally that failure by mechanical means can occur.

Introduction

The work described here is part of a project dealing with failure analysis of aircraft engine and accessory components carried out in the School of Chemical Engineering and Materials Science at the University of Oklahoma. The work is sponsored by the Oklahoma City Air Logistics Center,

AFLC, U.S. Air Force. Where documentation is available on the failure
history of a class of components or information is available on the service
conditions of a particular component, it is often possible to deduce the
circumstances leading to a specific failure. Otherwise, the analyses are
limited to characterizing the failure according to the basic mechanisms
that are indicated.

Corrosion as a causative or contributive agent to the process is
indicated in a large number of failures we have analysed. This paper presents
case studies of failures in three very different types of components which
appear to share the common thread of being corrosion-related failures.

Breech Chamber Failures

One of the most frequently failed components for which analyses have
been required is the breech chamber used in cartridge/pneumatic starters on a
variety of aircraft engines. The chambers are part of the pressure containing
system and hold a burning charge. The combustion products which are produced
are directed toward the turbine to effect a quick start of the engine.
Operating conditions typically involve a 20 second burn time, pressures in
the neighborhood of 700 psi and metal temperatures of about 1100°F. Failure
usually will produce damage to the neighboring engine and airframe structures
as the burning gases escape through a rupture in the system.

Two types of breech chambers have been examined in some detail. One type
is produced as an investment casting using the cobalt base alloy Stellite 21.
These chambers show only mechanical failures by overload at the bayonet
closure. There appears to be some question about the adequacy of the pressure
relief system in this group of components. However, no corrosion induced
failures have been observed. The second group of chambers is fabricated from
4340 steel heat treated to hardnesses in the range, Rockwell C 40 to 45.
Examination of failed components indicates that after some service the material
degrades to hardnesses in the neighborhood of Rockwell C 35. Stress analysis
indicates that the corresponding reduction in strength renders the design
marginal from a purely structural-mechanical standpoint.

Figures 1 and 2 show examples of typical failures in the steel breech
chambers. The dome blows out at a location opposite the hot gas discharge
nozzle. The failures occur in the region of highest stresses (according to
stress analysis) at the change in section where the dome meets the body of the
chamber. The photographs show the internal heat shields exposed by the
failure. The shields are not sealed to the discharge duct and are not pressure
containing components. Circulation of the cartridge combustion products can
occur around the shields making cleaning of the residues difficult and uncertain.

Analysis of the failures is often made difficult by flame erosion and
deterioration of the fracture surfaces. The changes produced obliterate
necessary details of the fracture origin. The internal surfaces of the
failed components are generally covered by a heavy layer of combustion
products and are generally degraded by corrosion. Figure 3 is a photo-
micrograph of a cross-section through the failed chamber wall adjacent to the
fracture origin. The photograph shows pitting of the internal wall. The
pitting was noted to be quite deep in some places. Figure 4 shows a higher
magnification view of the cross-section at the failure origin. One
may note jagged, branching cracks which appear to follow the prior austenitic

grain boundaries in the heat treated structure. Some of the cracks contained a heavy deposit of oxide scale indicating their existence over prolonged periods prior to the failure. The cracks shown in the photograph are reasonably clear of oxide indicating they are of relatively recent origin.

The internal surfaces of the chambers which are exposed to the combustion products are not coated for corrosion protection. The external surfaces, specifically the dome, are covered with a coating of electroless nickel. The logic of this design is not immediately obvious in view of the potential sources for the most serious corrosion attack. Further, it should be recognized that the coating is inherently quite brittle. As the chamber is used it is subjected to internal pressure and thermal stresses in each service cycle. These stresses induce brittle cracking of the coating as shown in Figure 5. Corrosion attack of the base metal was often noted to be associated with these cracks. Figure 6 shows a typical example. The corrosion observed is most probably the result of galvanic coupling of the more noble nickel coating with the active steel chamber. The galvanic corrosion process appears to be a slowly progressing failure mechanism which should be capable of inducing fracture in the absence of other more rapid processes. The other processes do operate and an externally induced failure has not been observed thus far.

A particularly striking example of galvanic corrosion produced by the nickel coating was exhibited by a chamber which failed due to a complete separation encircling the bayonet locking connector. This chamber also contained the fracture at the hot gas nozzle, shown in Figure 7. The failure appears as a brittle, jagged crack extending about halfway around the nozzle. The fracture is of the same character as the fractures shown in Figures 3 and 4. This crack morphology is usually taken as evidence of failure by stress corrosion cracking (SCC). On the external surface of the chamber there is a craze pattern of trenches that extends beyond the failure crack at the base of the nozzle, Figure 8. Figure 9 shows a cross-section through the trenches associated with the craze pattern.

In evaluating SCC problems it is traditional to try to identify the source of stress and the specific corrosive agent responsible for the failure. Here it may be recognized that the cartridge contains a variety of materials that are capable of inducing pitting and SCC. The charge is an ammonium nitrate-based material in an (acid) organic binder. The potential for damaging species exists in both the combustion residues and any unburned cartridge material which is deposited on the chamber walls. The combustion products are likely to be hygroscopic and their deposition on inaccessible areas of the chamber further compounds the problem.

The most probable source of persistent stress (leading to SCC) is derived from the thermal cycles the chamber experiences. The rapid changes in body cross-section are conducive to uneven heating and cooling of the metal and localized regions of high stress due to notch effects. These are further intensified by pitting attack and general corrosion which acts to raise the local stresses. Finally, degradation of the strength properties of the metal also would contribute to catastrophic failure of the assembly.

Exhaust Tailcone Assembly

An unusual problem for which failure analysis was required involved the separation of a portion of the exhaust tailcone from an A-7D aircraft. About one-third of the assembly fell away from the airplane during a flight over Pittsburgh, Pennsylvania and the part was never recovered. Figure 10 shows an overall view of the portion of the cone that remained. The original cone tapered from about three to two feet in diameter, was about six feet long and was formed from sheet approximately 0.020 inches in thickness. The structure was stabilized with circumferential stiffeners on the outside. The piece that fell off in-flight was large enough to do considerable damage.

Figure 11 shows one of the stiffeners. Failure occurred in the body of the tailcone adjacent to the stiffener. Figure 12 details the stiffener which is resistance welded to the body in a skip or stitch weld pattern. The continuous longitudinal weld used to join the body is shown in Figure 13. The body material is A-286, a precipitation-hardened iron-base superalloy.

The contour of the fracture surface which encircled the body of the tailcone indicated that the origin of the failure occurred at the junction between the longitudinal and circumferential welds. Figure 14 and 15 are scanning electron micrographs of the fracture surface near the failure origin. As demonstrated by the photographs the majority of the failure exhibited dimple rupture evidencing failure due to simple overload. More detailed examination, in this same area revealed a pattern of metal degradation on the inside surface of the tailcone. Figures 16 and 17 show a network of coarse and fine cracks extending into the metal.

A cross-section was made through the junction of the longitudinal weld in the body and the circumferential stiffener weld at the stiffener adjacent to the large end of the cone (shown in Figure 10) where no failure had occurred. Figure 18 shows a photomicrograph of the weld nugget and the parent metal from both the stiffener and the body. In the more detailed view of Figure 19 one may note severe intergranular degradation of the weld which has isolated many of the metal grains. Figures 20 and 21 show intergranular attack of the parent metals.

The jagged, branched character of the cracks shown in the photomicrographs are indicative of stress corrosion cracking. The geometry of the tailcone configuration at the failure origin appears to be capable of producing the persistant stresses required for SCC. The crossing of a longitudinal and a circumferential weld would normally result in residual stresses when the metal cooled from the final weld. These stresses may not anneal out at the temperatures produced during normal use of the assembly.

The photomicrographs also demonstrate that the structure as revealed by electrolytic oxalic acid etching shows clearly defined grain boundaries or the "trench" type structure defined by ASTM A-262. The metal is thus shown to be disposed toward intergranular corrosion because of precipitate formation in the grain boundaries. The specific agent responsible for crack formation was not determined, but may be assumed to be a component of the engine exhaust gas stream.

Hydraulic Cylinders

The last class of component failures to be discussed involves various types of hydraulic cylinder bodies. Figure 22 shows an overall view of the inner landing gear door actuator cylinder from an F-101 aircraft. The material was reported to be 2024-T4 aluminum; this was verified by chemical analysis and hardness measurement. Figure 23 shows a close up view of a through wall crack in the cylinder. The metal surface is pitted and there is evidence of an identification band having been located in this area. The bands are typically attached with a rubber-like adhesive material.

Figure 24 shows the fracture surface associated with the crack. The area shown is believed to be the origin of the failure. Here the metal exhibited a "woody" appearance. A more detailed view of this area, revealed by SEM is presented in Figure 25. The metal shows the results of corrosion attack and typical exfoliation damage. It appears likely that this damage initiated the failure process. Areas of the fracture surface adjacent to the origin showed clear evidence of fatigue striations (Figures 26 and 27) obviously introduced as the cylinder was pressure cycled in use.

Transverse cross-sections through the cylinder beneath the banded area showed incipient cracks extending from the outside surface inward. It is a crack of this type that is presumed to have caused the failure. There are some well recognized dangers associated with the partial isolation of metal surfaces exposed to oxygenated corrosion media. Metals are susceptible to corrosion damage due to differences in oxygen concentration across the exposed surfaces. Moisture permeable films act to partially isolate the metal from oxygen in the environment and become preferred sites for corrosion attack. The process is often called differential aeration attack. The effect is much more pronounced with metals like aluminum that depend upon oxygen for production and repair of a normally protective surface film. Under conditions of oxygen deprivation the passive film may become damaged and the metal will be susceptible to rapid pitting attack.

A number of failures were studied all of which appeared to be associated with identification bands attached to hydraulic cylinders. Figure 28 shows the main landing gear actuating cylinder from a C-141 aircraft. The material is 2014-T6 aluminum. The closer view of the surface shown in Figure 29 shows a crack which has opened in the wall beneath the band. Figure 30 shows an area of the surface where a small piece of metal was lost either because of a forging defect or because it was isolated by corrosion. The appearance of a normal, overload fracture in the cylinder wall (Figure 31) may be compared with the fracture surface near the failure origin (Figures 32 and 33). The latter exhibits the same woody appearance which characterizes exfoliation attack. Here again attack was induced by differential aeration and was the result of a band attached to the cylinder surface. Once initiated, failure proceeded by fatigue as evidenced by the striations shown in Figure 34.

A similar type of failure was found in another C-141 hydraulic cylinder. The woody, darkened area on the fracture surface at its origin was examined with the electron probe microanalyser. This area was found to contain a number of contaminents, including chlorine, potassium and calcium. These are considered significant indications of water residues and particularly damaging species to which aluminum is susceptible.

Conclusions

The case histories discussed above present examples of corrosion due to relatively simple and well known mechanisms. Corrosion as a potential source of failure obviously must be acknowledged along with mechanical considerations in the design and maintenance of aircraft accessory components.

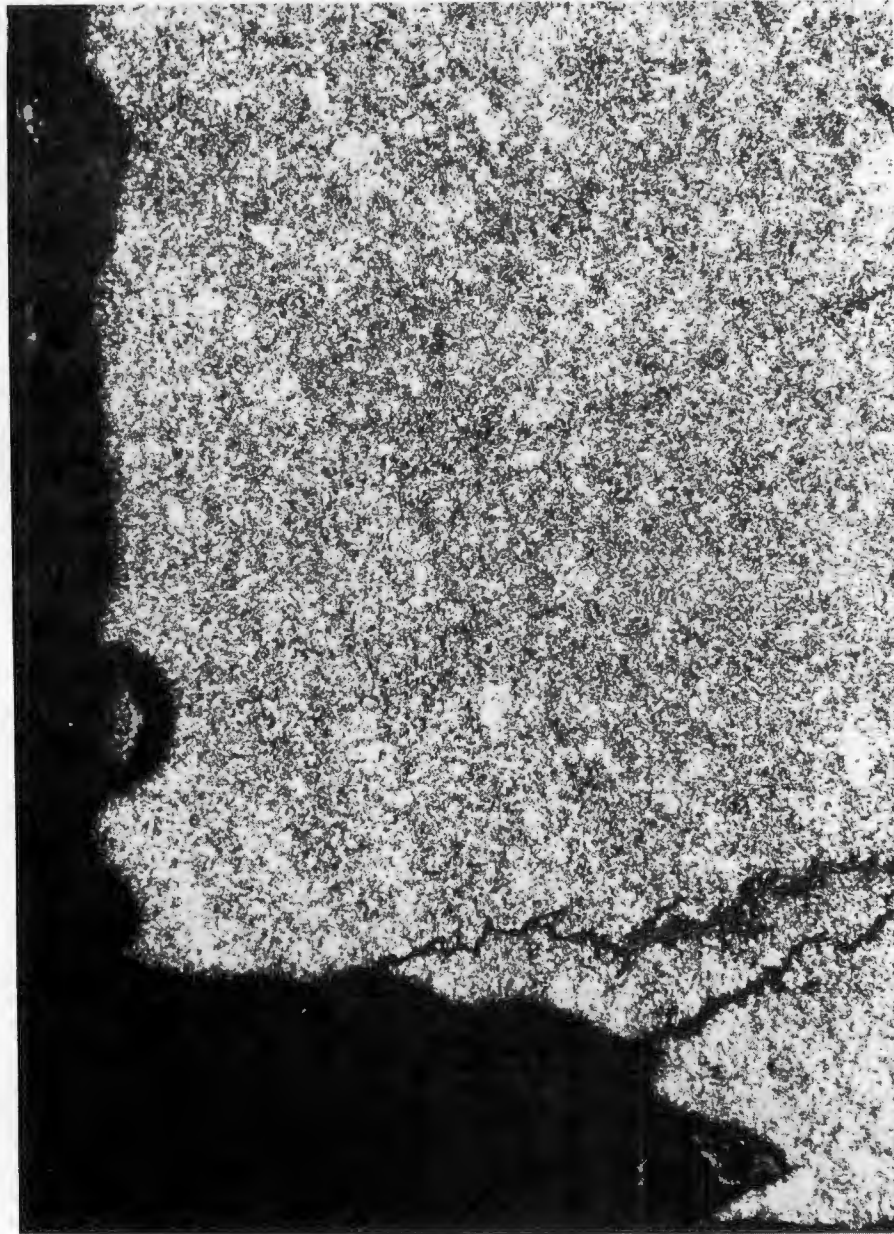Figures 1 (above) and 2. Breech chambers which have suffered dome blowout failures.

Figure 3   150 X   Nital-Picral Etch

Photomicrograph of a cross section through the
breech chamber wall. Internal wall (left ver-
tical edge) exhibits a pitted surface. Prior
austenitic grain boundaries are outlined by a
jagged crack.
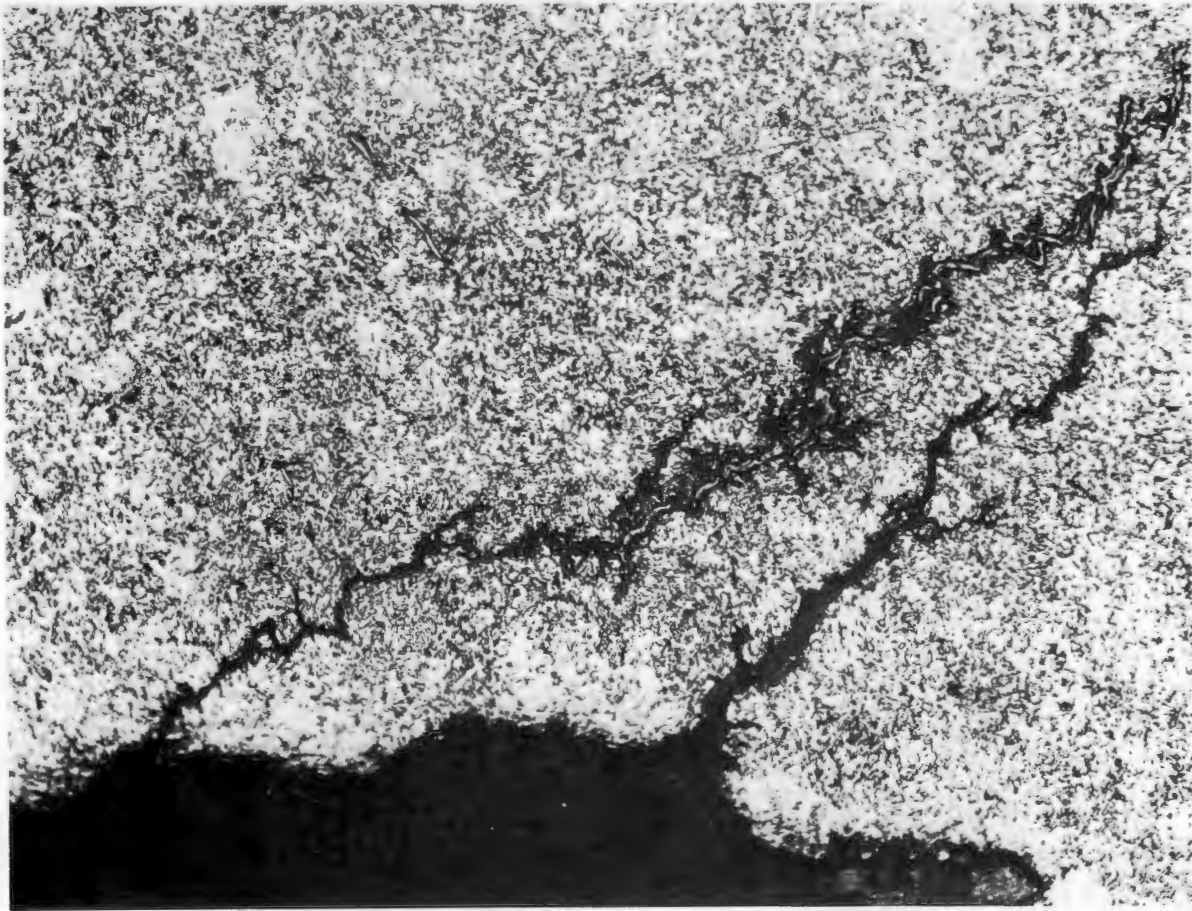
Figure 4   300 X   Nital-Picral Etch

High magnification view of the jagged crack shown in Figure 3.
The stress corrosion crack winds through a microstructure of
tempered martensite; hardness Rockwell C 35.
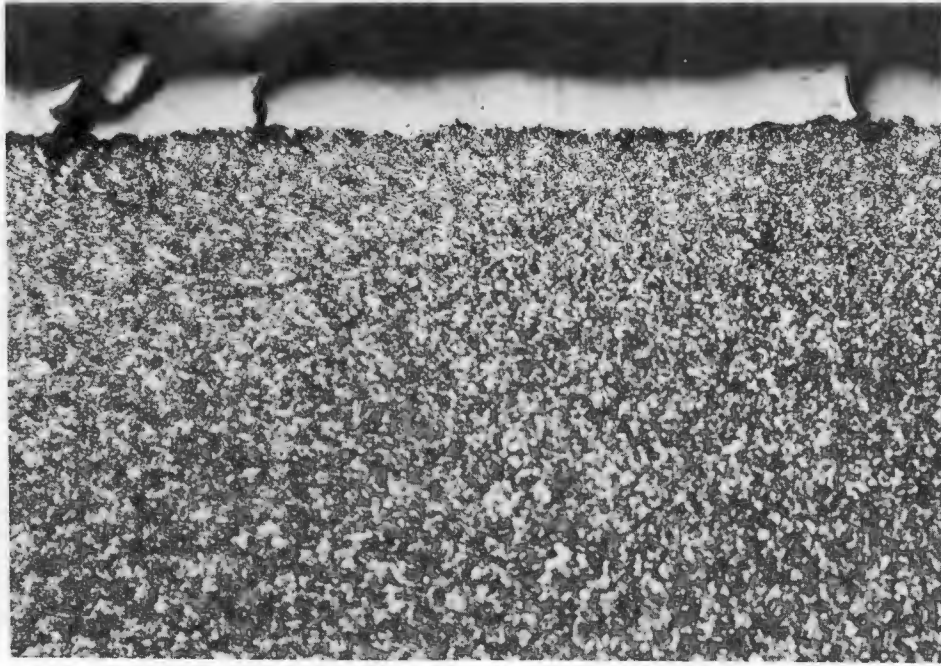
Figure 5   300 X   Nital-Picral Etch
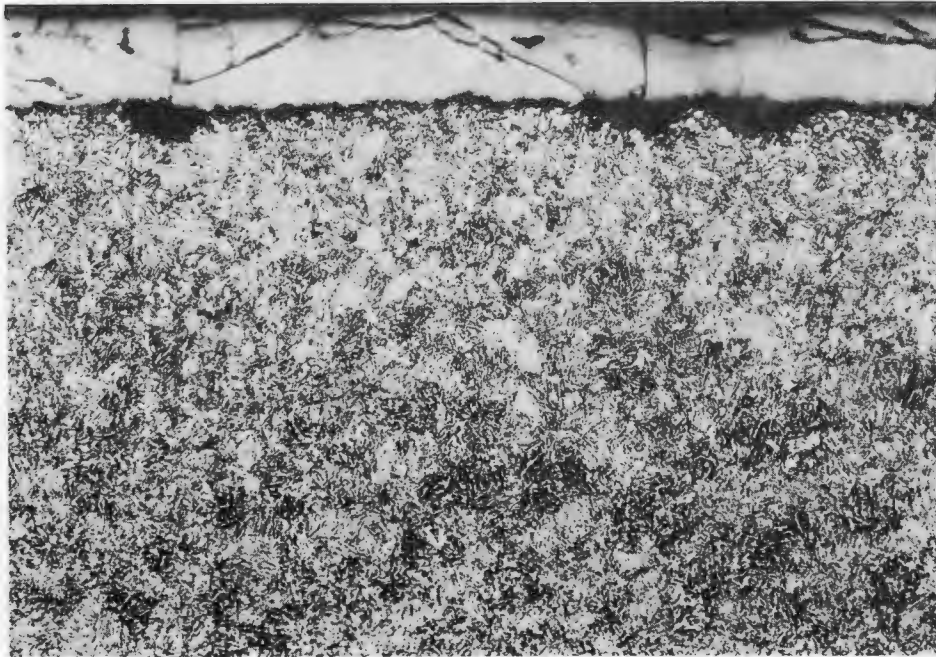
Figure 6   300 X   Nital-Picral Etch

Photomicrographs revealing nature of brittle nickel coatings.

Figure 7.   Fracture encircling the hot gas nozzle of
a chamber which has also failed in the bayonet lock.
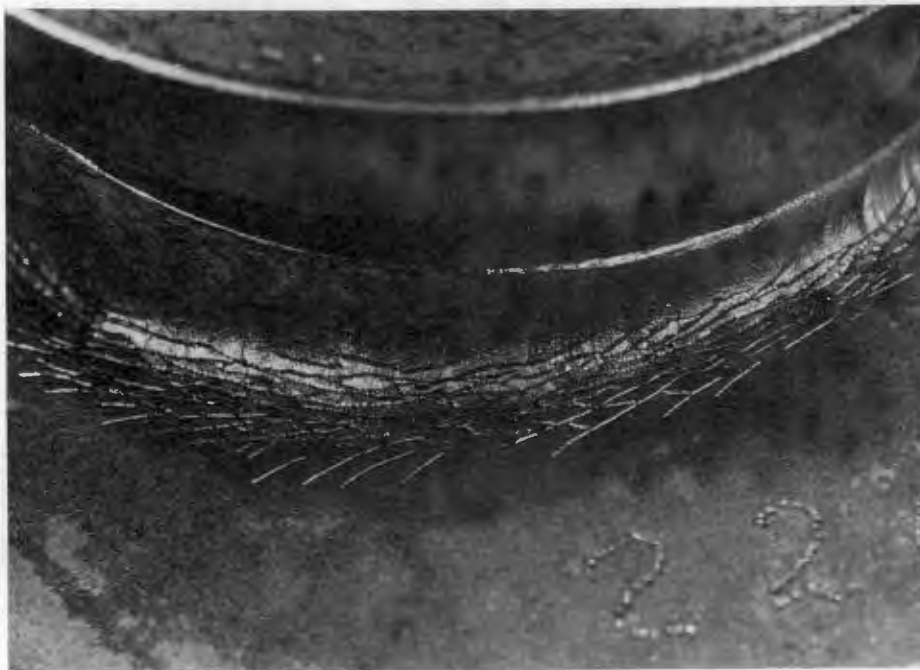
Figure 8.   Craze pattern of trenches extending beyond
the main failure and at the base of the nozzle.
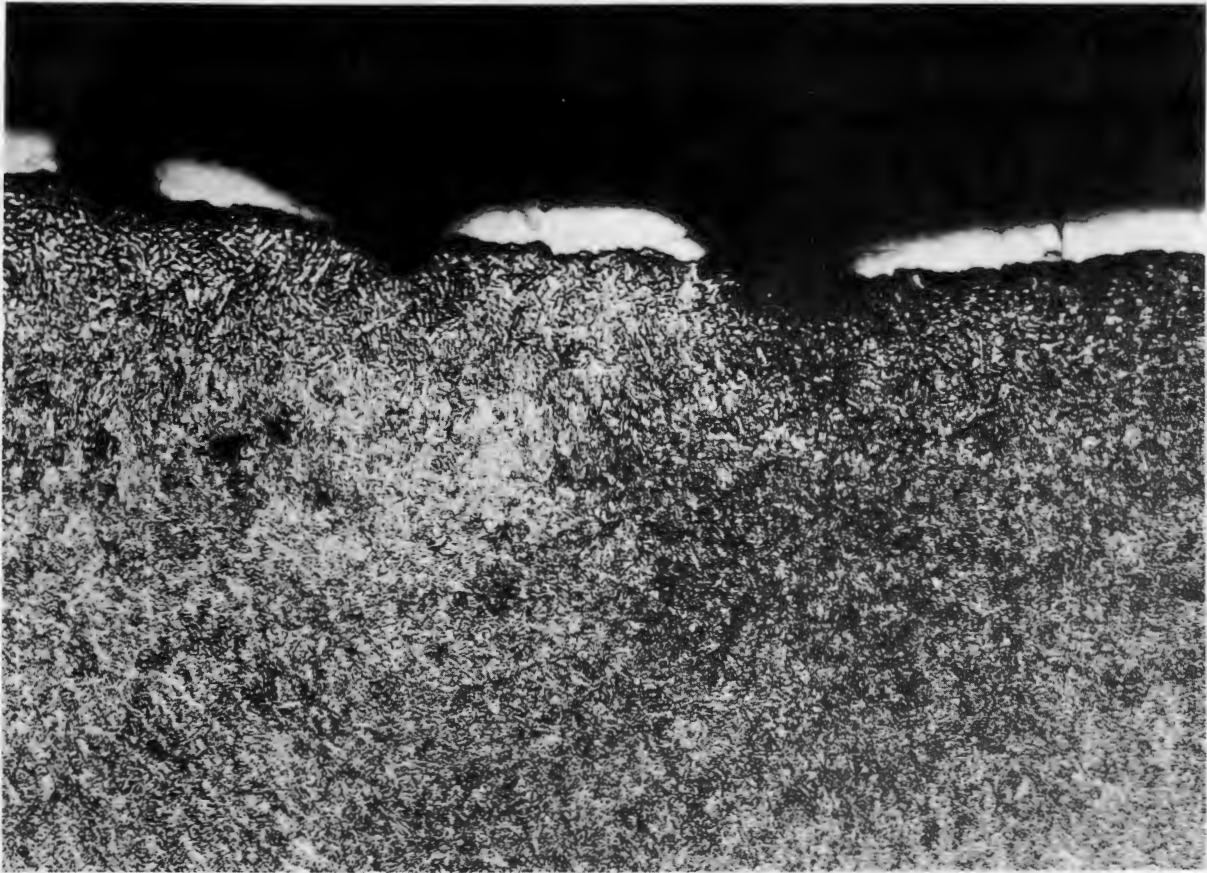
Figure 9   300 X   Nital-Picral Etch

Cross section through the trenches associated with the craze
pattern identified in Figure 8.

Figure 10.   Overall view of the separated
tailcone assembly. A-7D aircraft.

Figure 11.   Close up view of the tailcone stiffener.
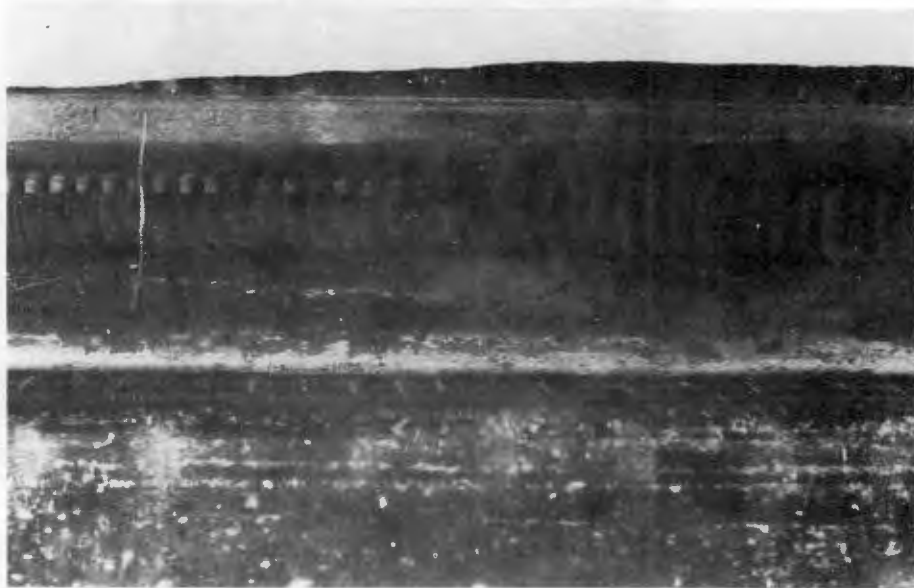
Figure 12.   Detail of stiffener showing resistance stitch weld.
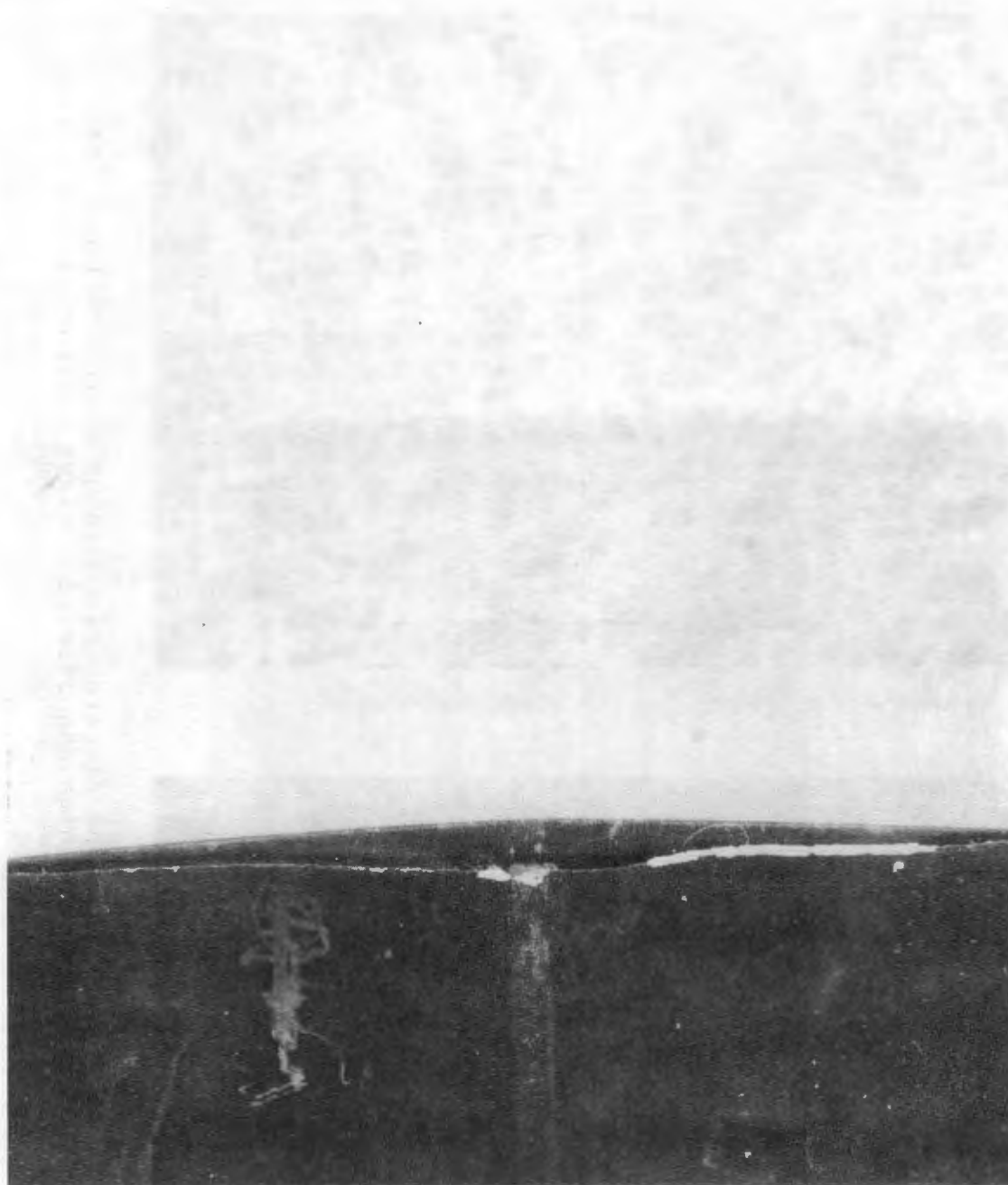
Figure 13.   Continuous longitudinal weld used
to join the body.
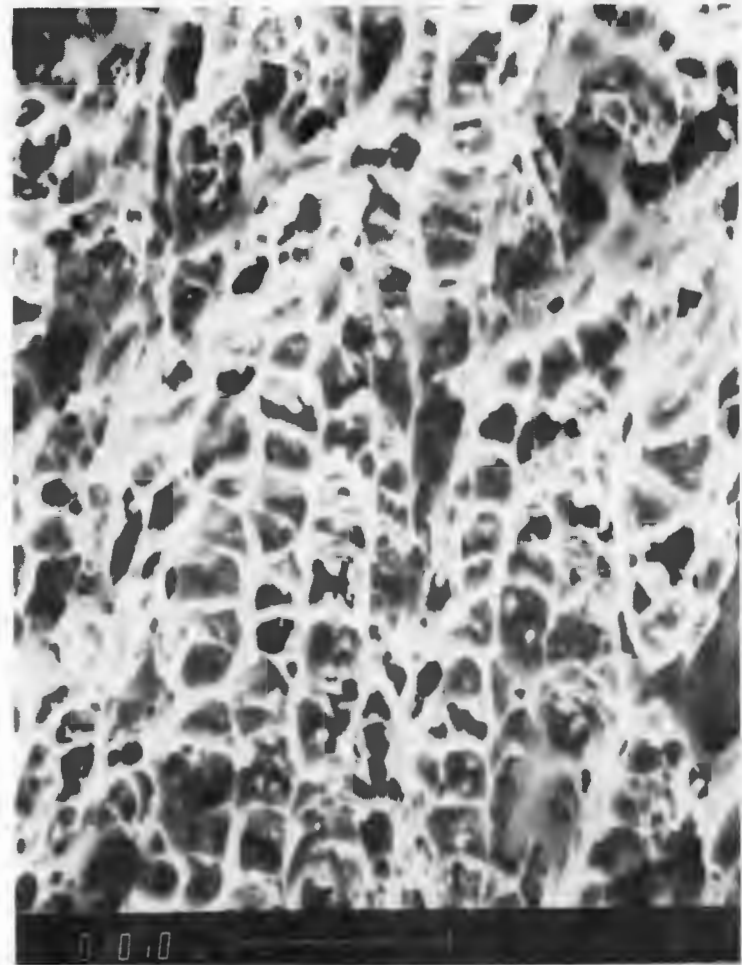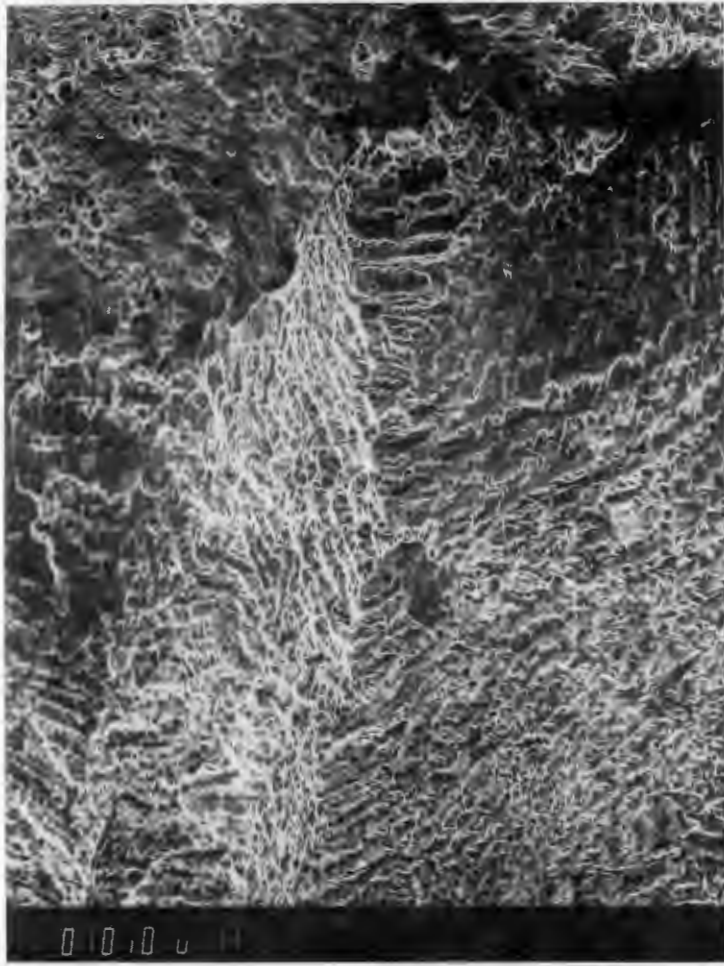
Figures 14 (left) and 15.   Scanning electron micrographs of the tailcone fracture near the failure origin. Low and high magnification views indicating dimple rupture due to simple overload.
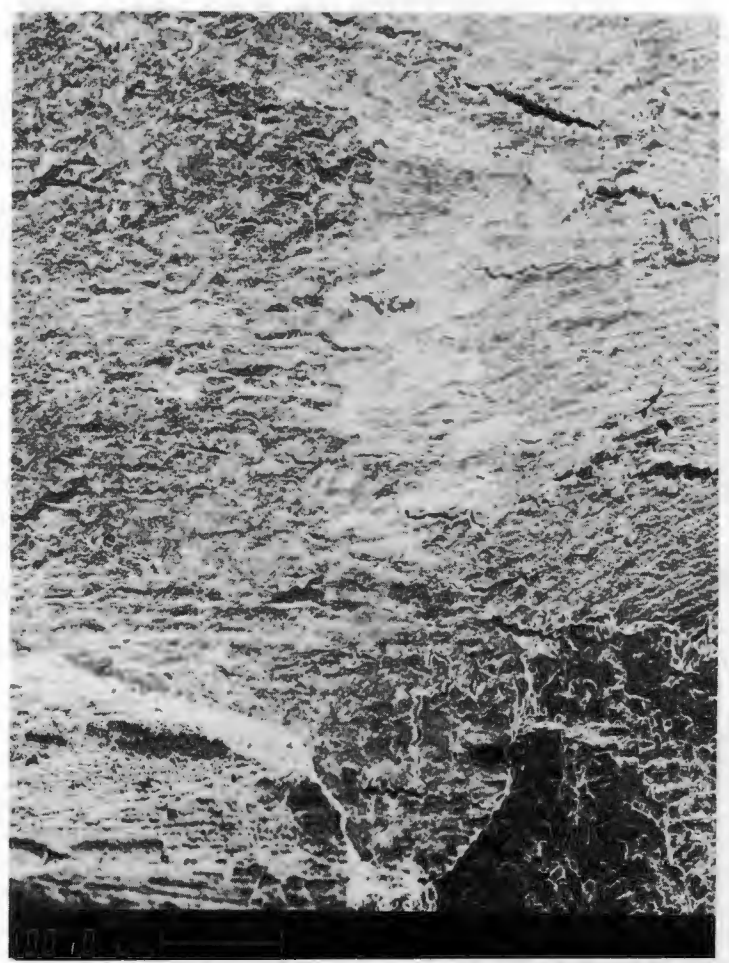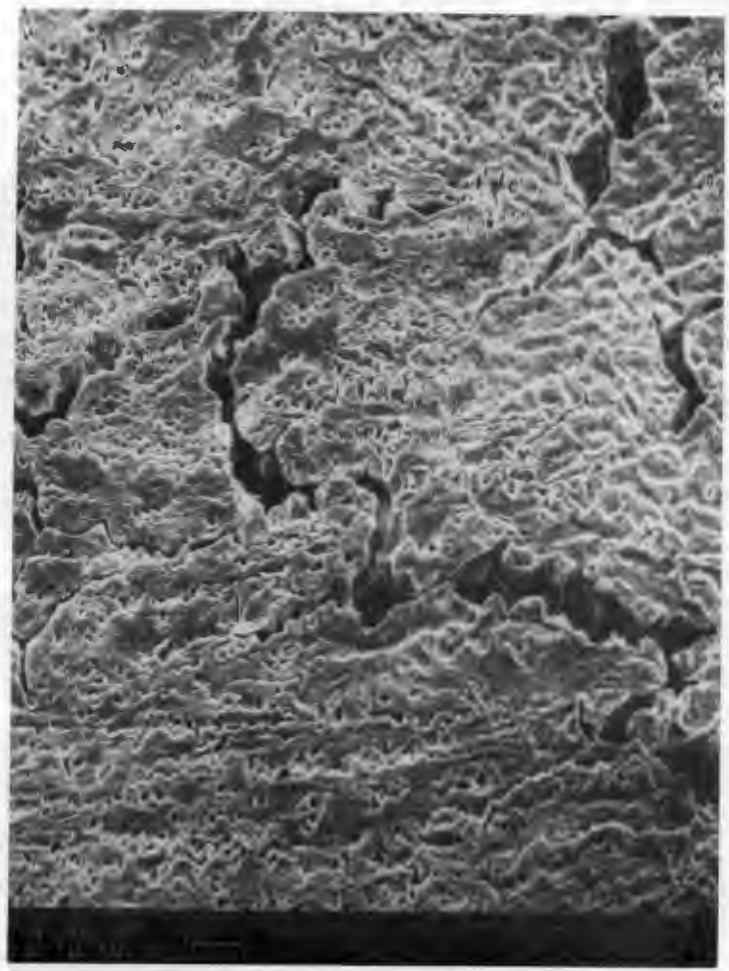
Figures 16 (left) and 17.   Low and high magnification scanning electron micrographs
showing crack network adjacent to the failure extending into the metal wall.
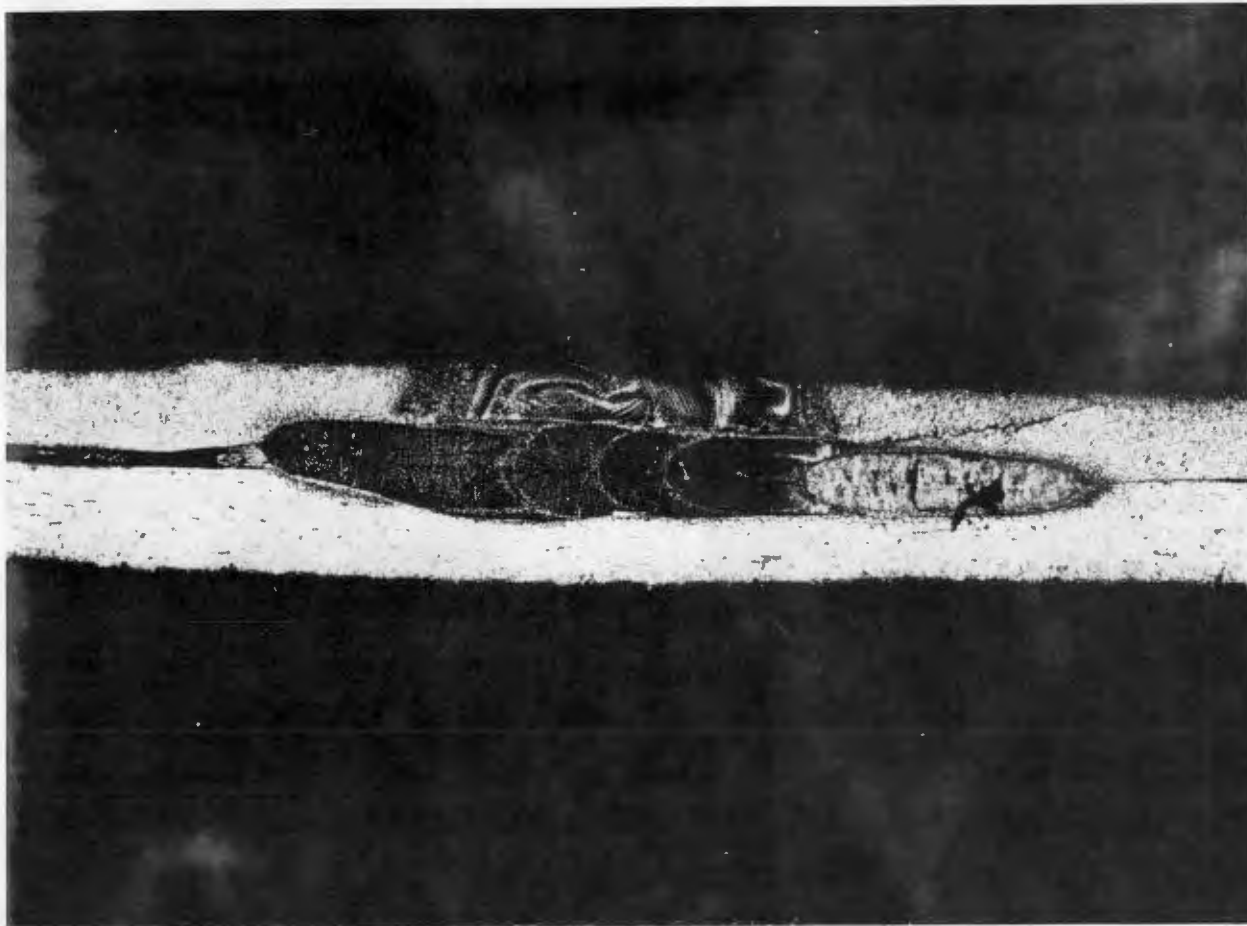
Figure 18   230 X   Electrolytic: 10% Oxalic Acid

Weld nugget and parent metal from the stiffener and the body.
Figures 19 and 20 show high magnification views taken near the
left extreme of the weld nugget.

Figure 19   100 X   Electrolytic: 10% Oxalic Acid
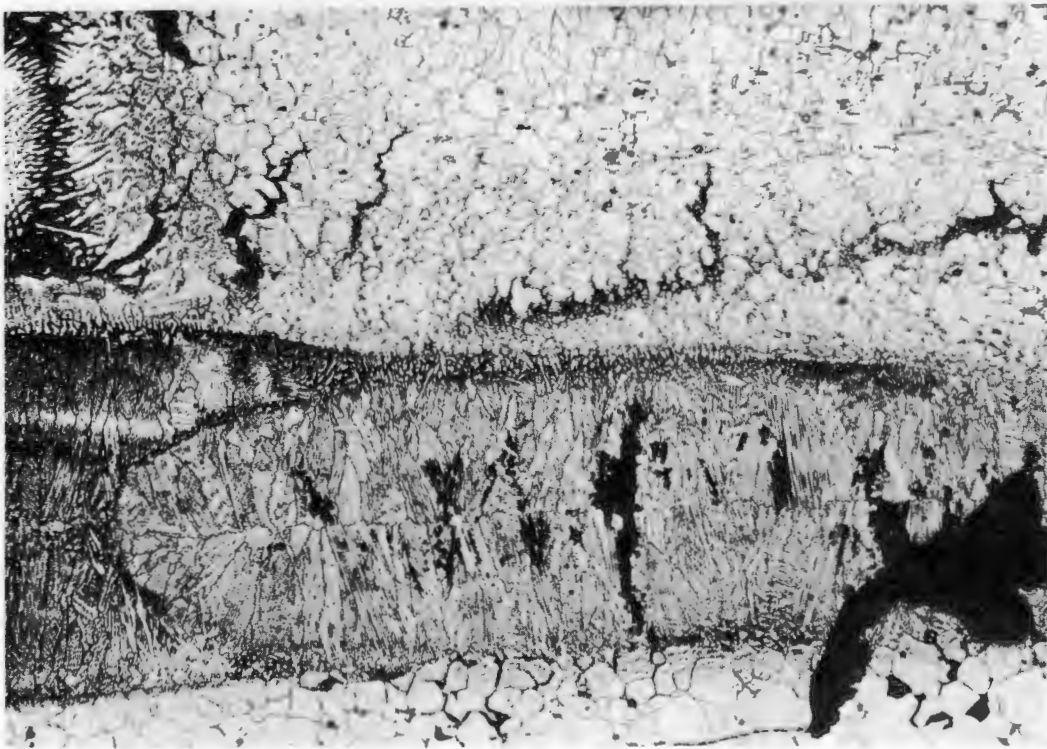
Figure 20   130 X   Electrolytic: 10% Oxalic Acid

Severe intergranular degradation of the weld and parent metal.
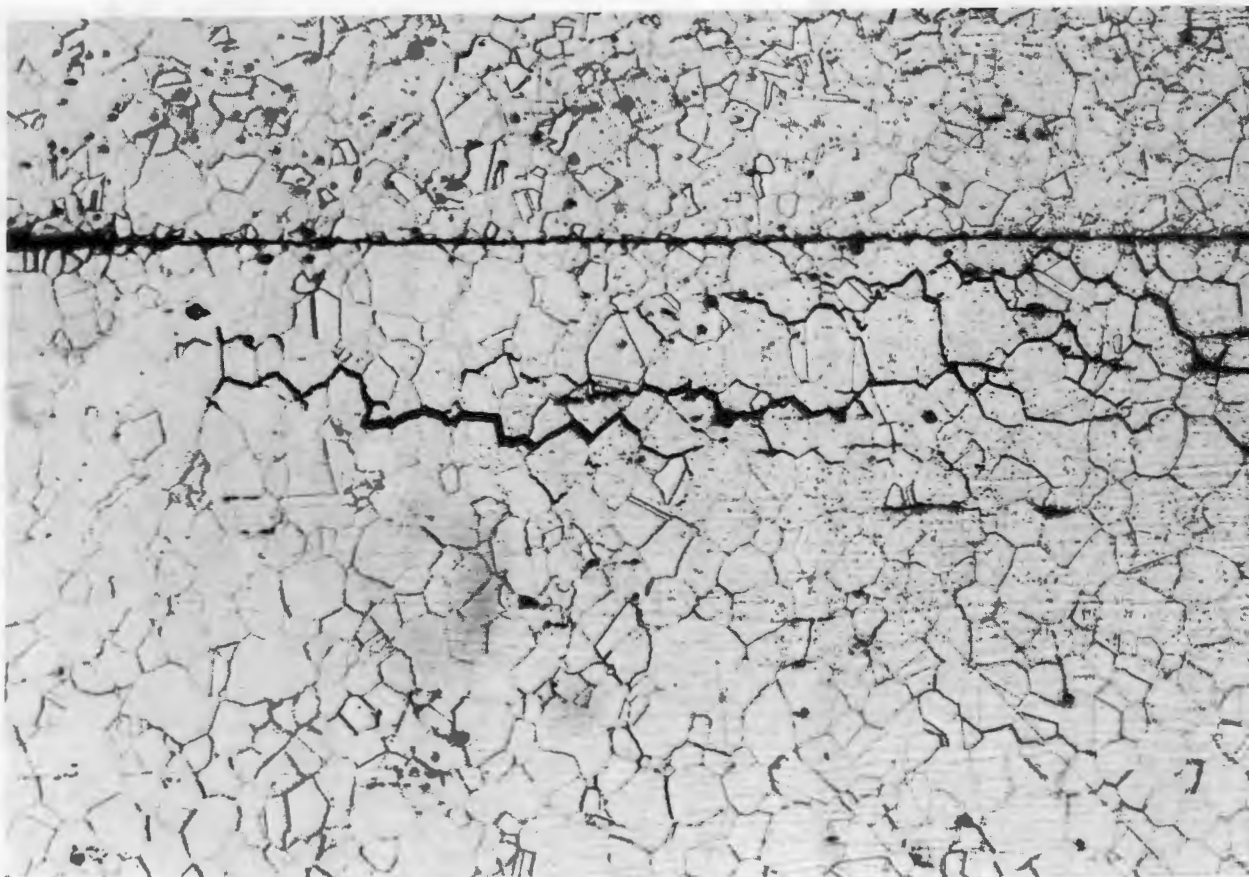
Figure 21   200 X   Electrolytic: 10% Oxalic Acid

Intergranular attack extending outward in directions opposite of
the weld nugget.
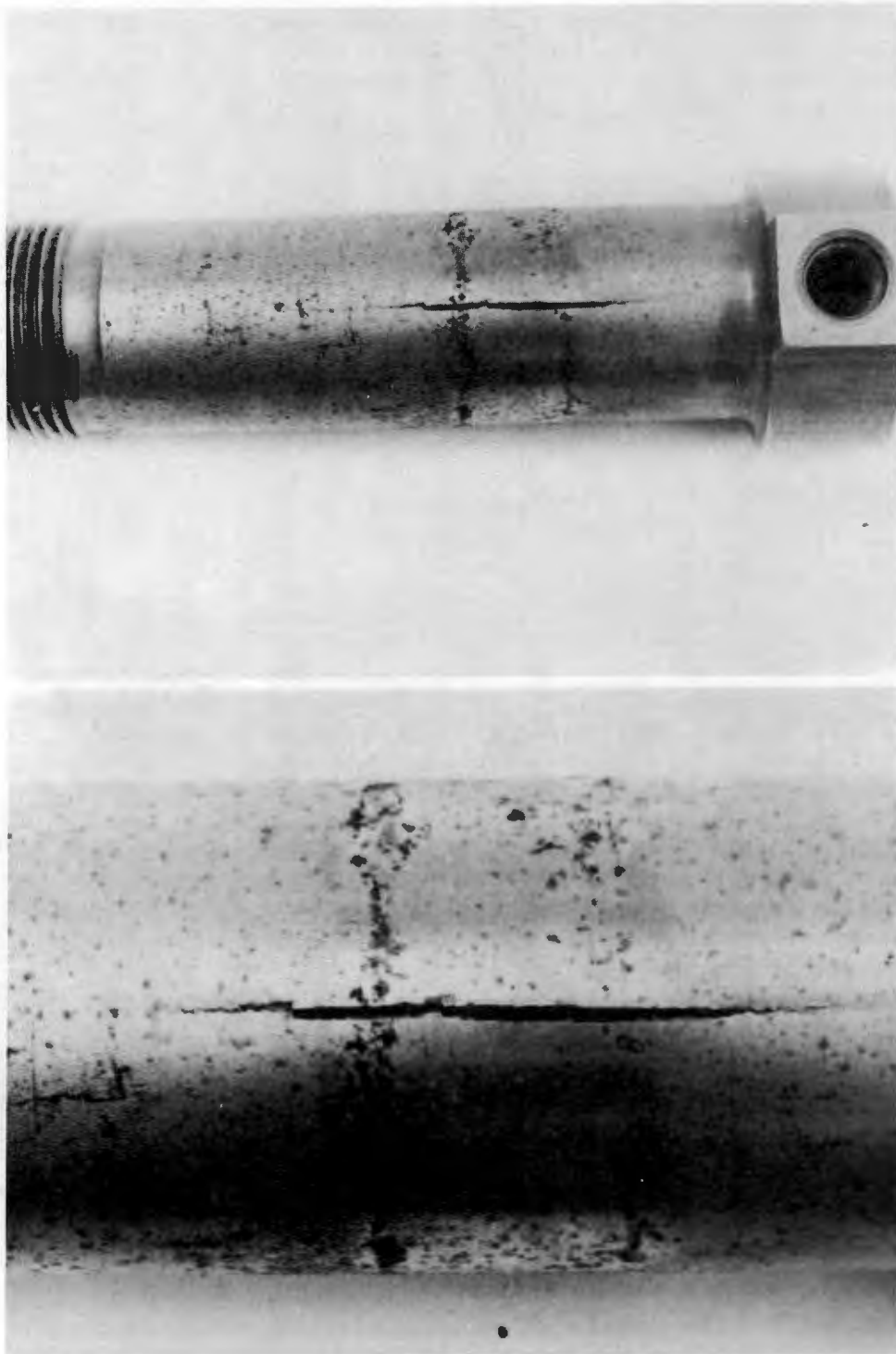
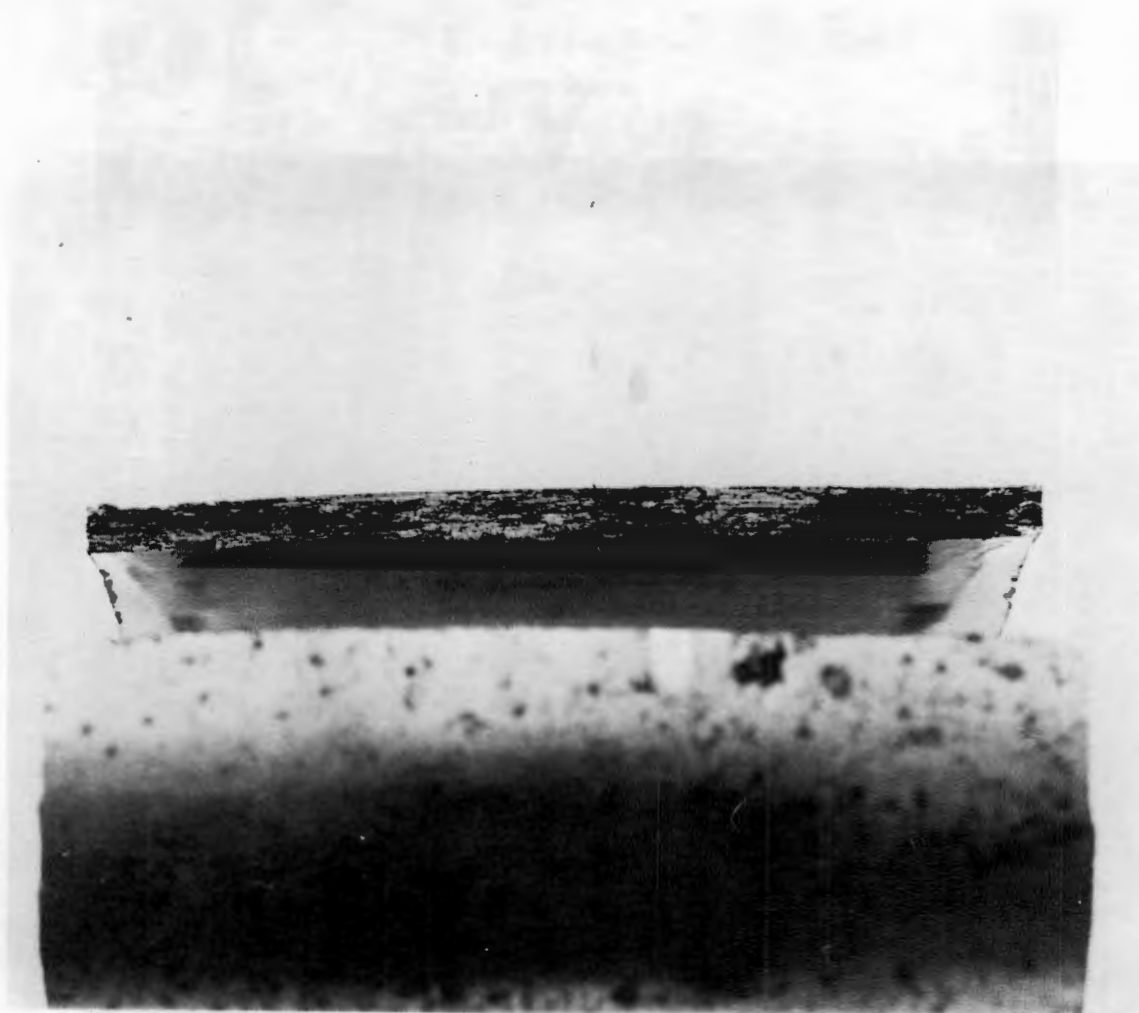Figures 22 (above) and 23. Selected views of the inner landing gear actuator cylinder exhibiting a failure oriented longitudinally in the cylinder wall.
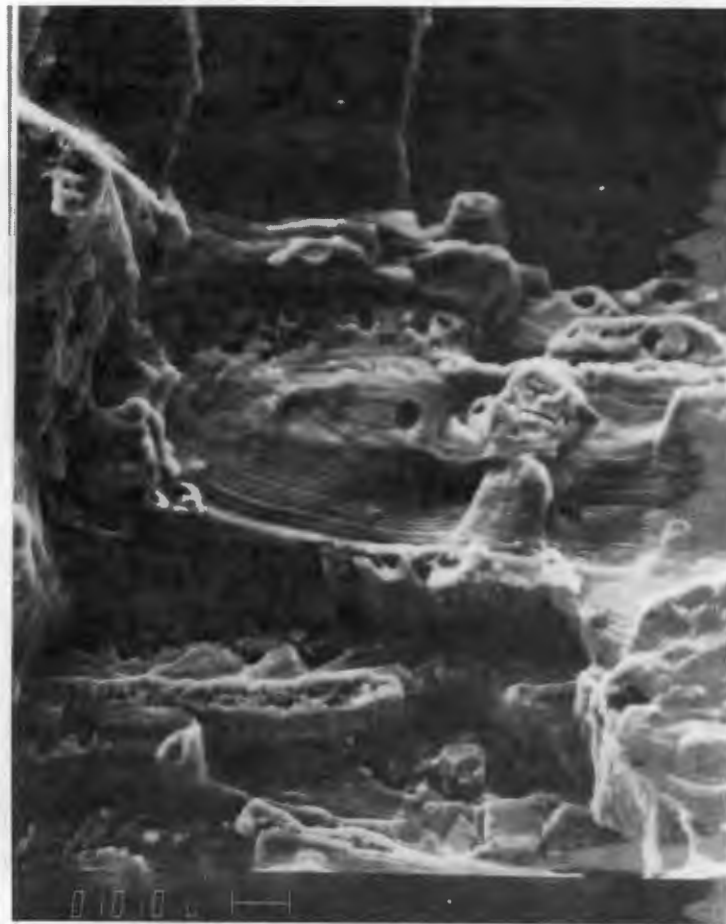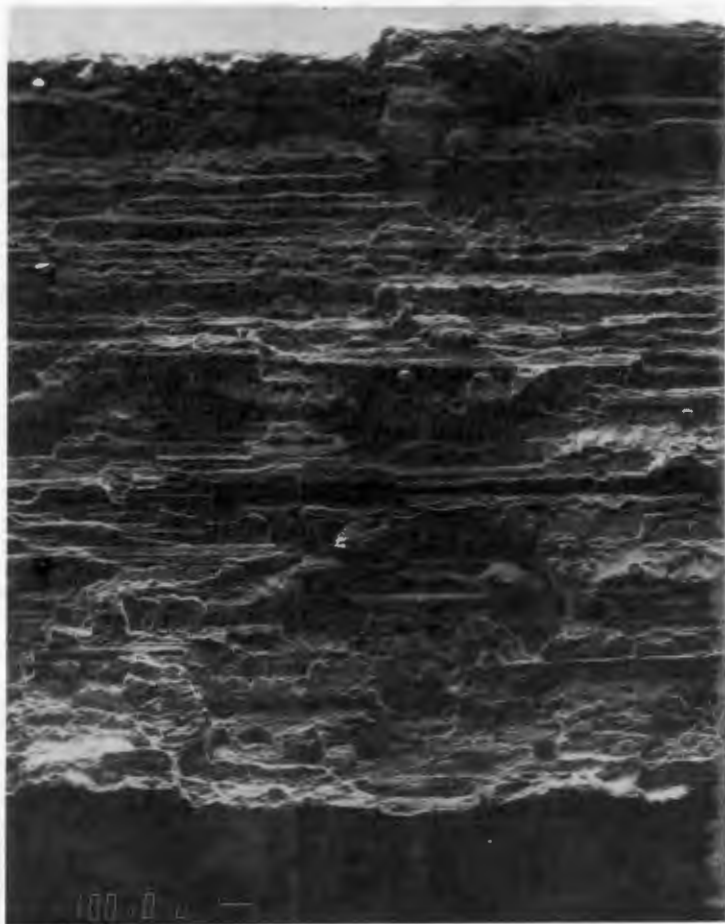
Figure 24.   Fracture surface associated with the longitud-
failure in the cylinder wall.

Figures 25 (left) and 26.   SEM views of the fracture surface shown in Figure 24.
"Woody" features dominate the image in Figure 25 which appeared to have initiated
the evidence of fatigue failure in Figure 26.

Figure 27.   Another view of fatigue
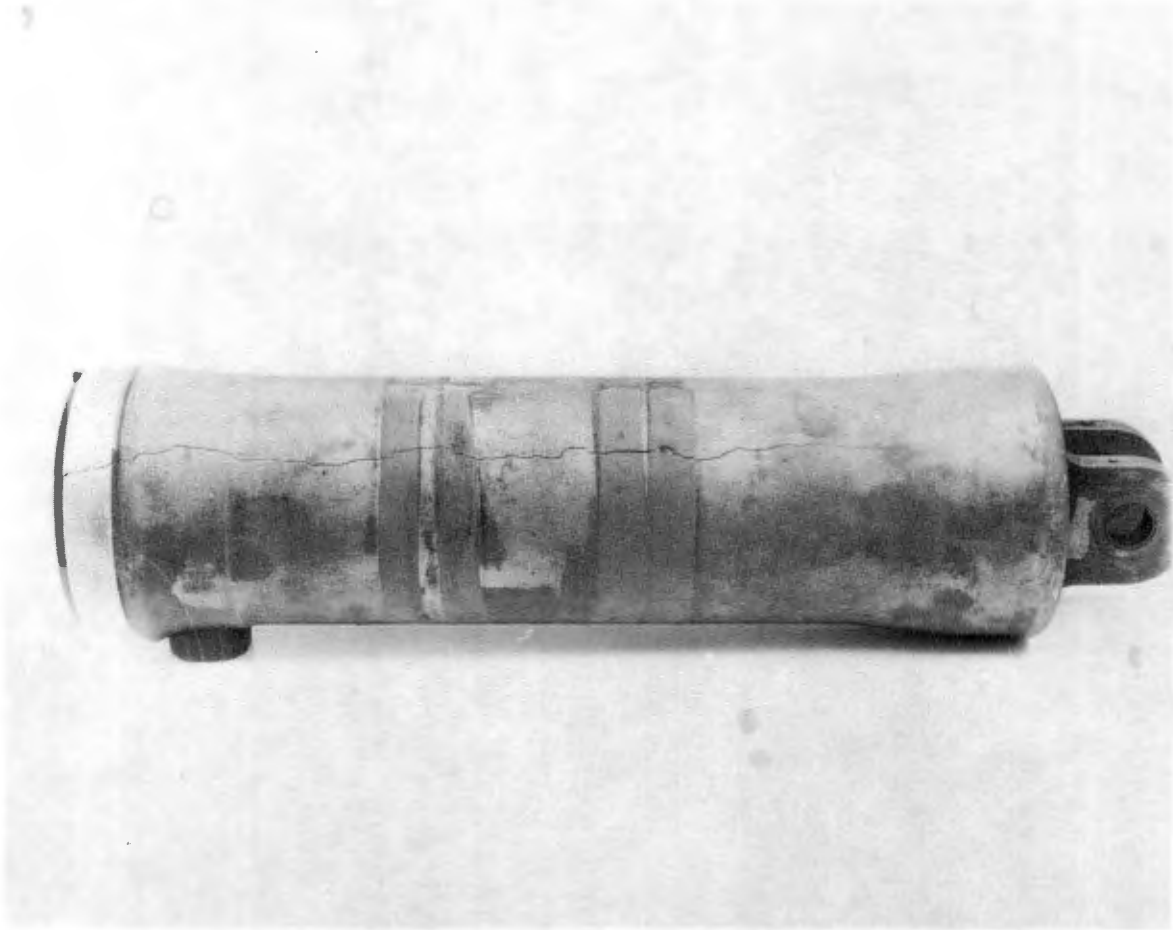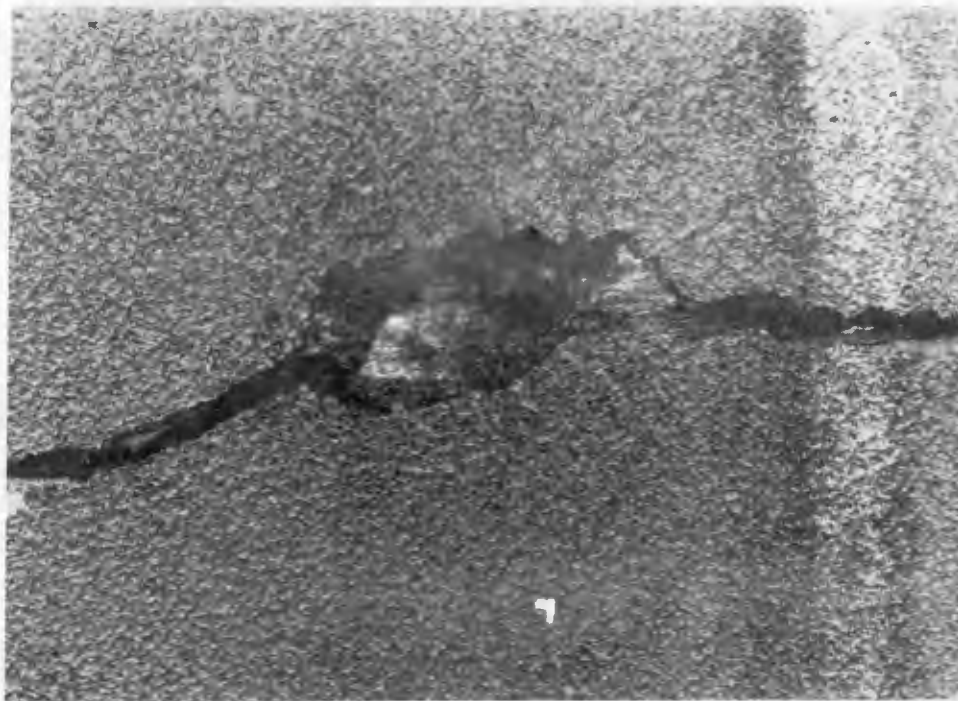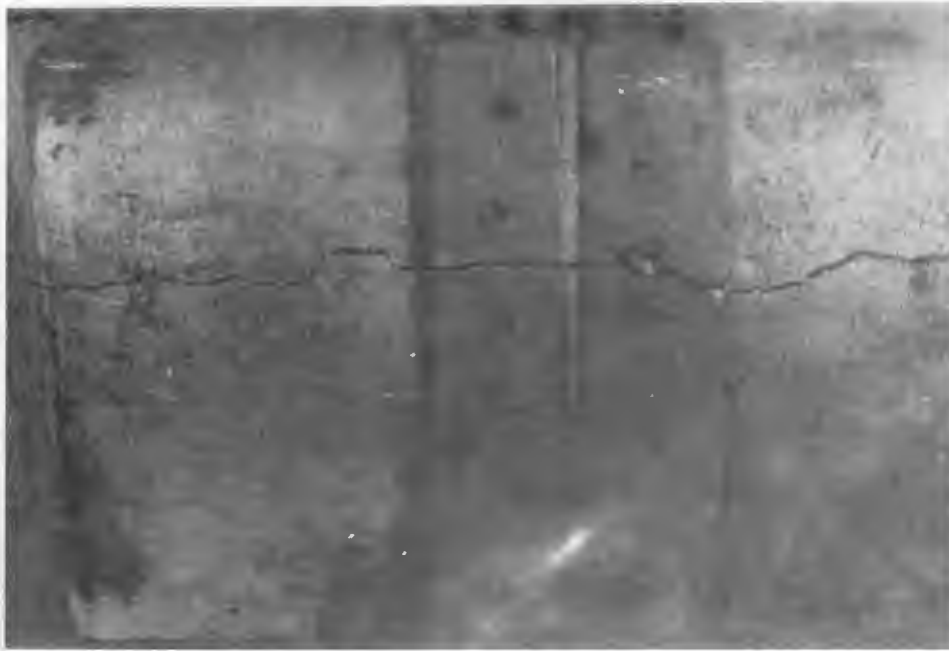striations in the cylinder wall.

Figure 28.   Overall view of the failed main landing gear
cylinder.   Note the anomaly in the wall.

Figures 29 (above) and 30.   Close up views of the
fracture in the longitudinal wall. Note the light
stripes around the outside diameter in Figure 29.

266

Figures 31 (above) and 32.   Areas in the failed wall
exhibiting different fracture modes. Normal ductile
failure remote from the origin (Figure 31) contrasted
with a laminated or exfoliated character in the vicin-
ity of the origin (Figure 32).

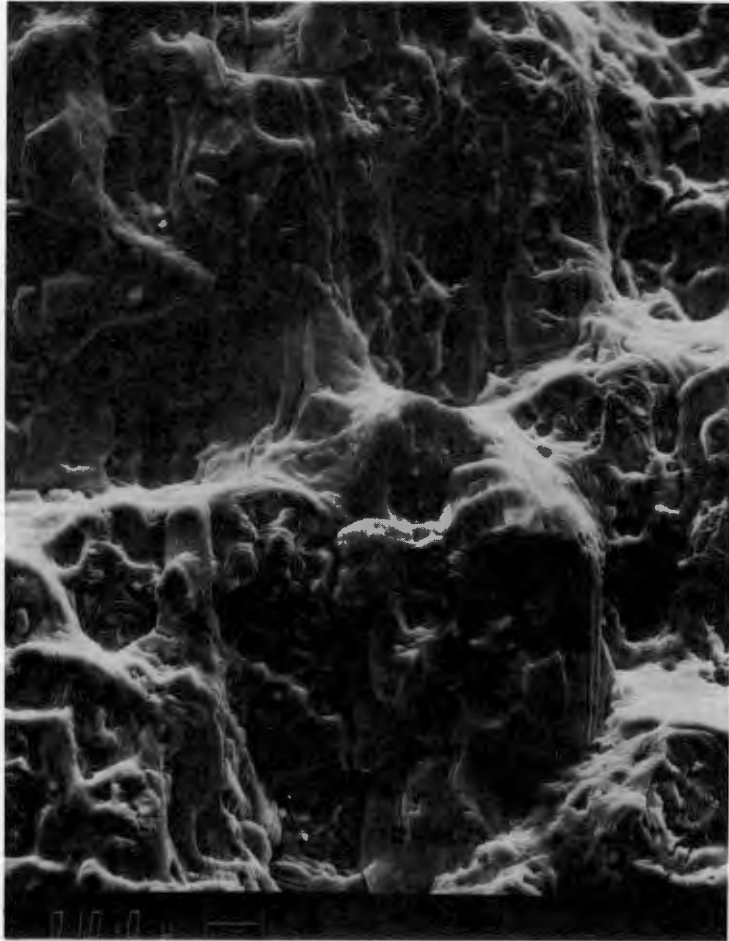Figure 33. Example of exfoliation attack near the failure origin. Again characterized by the laminations in the wall.

Figure 34.   Fatigue within the lam-
inated areas of the cylinder wall.

WILLIAM R. COLEMAN, Ph.D. candidate in Metallurgical Engineering
    School of Chemical Engineering and Materials Science, University
    of Oklahoma. Mr. Coleman earned the B.S. and M.S. in Metallur-
    gical Engineering from the University of Oklahoma in 1978 and
    1979. His research currently involves surface effects in crystal
    plasticity, heat treatment processes, and failure analysis.

ROBERT J. BLOCK, Professor of Chemical Engineering and Materials
    Science, University of Oklahoma. Dr. Block earned the B.S.
    in Metallurgy from the Massachusetts Institute of Technology
    in 1956, and the Ph.D. from the University of Illinois in 1963.
    Dr. Block has been on the faculty of the University of Oklahoma
    since 1963. His research interests include crystal plasticity
    and surface effects on plastic deformation. He is a frequent
    consultant on problems involving failure analysis and product
    liability.

RAYMOND D. DANIELS, Professor of Chemical Engineering and Materials
    Science, University of Oklahoma. Dr. Daniels earned the B.S.
    (1950) and M.S. (1953) in physics, and the Ph.D. in Metallurgy
    (1958), all from Case Western Reserve University. He has been
    employed by the National Bureau of Standards and the Union
    Carbide Corporation. He has been on the faculty of the Univer-
    sity of Oklahoma since 1958. His research interests include
    hydrogen embrittlement of metals and corrosion. He is presently
    serving on the Board of Directors of the National Association of
    Corrosion Engineers.

COLEMAN   BLOCK   DANIELS